Surface diffusion of *n*-alkanes on Ru(001)

Cite as: J. Chem. Phys. **92**, 5136 (1990); https://doi.org/10.1063/1.458547
Submitted: 12 September 1989 . Accepted: 08 December 1989 . Published Online: 31 August 1998

J. L. Brand, M. V. Arena, A. A. Deckert, and S. M. George

Surface diffusion of *n*-alkanes on Ru(001)

J. L. Brand,[a] M. V. Arena, A. A. Deckert,[b] and S. M. George
Department of Chemistry, Stanford University, Stanford, California 94305

(Received 12 September 1989; accepted 8 December 1989)

The surface diffusion of *n*-alkanes on Ru(001) was measured using laser-induced thermal desorption (LITD) techniques. The surface diffusion coefficients for propane, *n*-butane, *n*-pentane, and *n*-hexane all displayed Arrhenius behavior. The surface diffusion activation energies increased linearly with carbon chain length from $E_{dif} = 3.0 \pm 0.1$ kcal/mol for propane to $E_{dif} = 4.8 \pm 0.2$ kcal/mol for *n*-hexane. In contrast, the surface diffusion preexponentials remained nearly constant at $D_0 \simeq 0.15$ cm^2/s. Measurements performed at different coverages also revealed that the surface diffusion coefficients were coverage-independent for all the *n*-alkanes on Ru(001). The surface corrugation ratio Ω was defined as the ratio of the diffusion activation energy to the desorption activation energy, $\Omega = E_{dif}/E_{des}$. The surface corrugation ratio was observed to be remarkably constant at $\Omega \simeq 0.3$ for all the *n*-alkanes. This constant corrugation ratio indicated a linear scaling between the diffusion activation energy and the desorption activation energy. This behavior also suggested that the *n*-alkanes move with a rigid configuration parallel to the Ru(001) surface.

I. INTRODUCTION

The diffusion of molecules on single-crystal surfaces is a central issue in surface chemistry and physics.[1] Surface diffusion uniquely probes the underlying adsorbate–surface and adsorbate–adsorbate potentials.[1-3] Surface mobility also may be the rate-limiting step in many surface kinetic processes. Unfortunately, very few surface diffusion studies have been performed because of experimental difficulties. This shortage is particularly noticeable on metal surfaces because surface mobility may influence the kinetics of heterogeneous catalysis.

This paper examines the surface diffusion of *n*-alkanes on Ru(001) using laser induced thermal desorption (LITD) techniques. Studies of hydrocarbons on transition metal surfaces are important for an understanding of catalytic hydrogenation, dehydrogenation and Fischer–Tropsch synthesis.[4] Ru(001) is a model Group VIII transition metal surface that is particularly effective in Fischer–Tropsch hydrocarbon synthesis.[5-7] Likewise, the *n*-alkanes form a homologous molecular series of hydrocarbons where the carbon chain length can be varied systematically.

By progressively increasing the carbon chain length, the kinetics of surface diffusion and desorption were measured for propane, *n*-butane, *n*-pentane, and *n*-hexane on Ru(001). These investigations revealed a simple scaling between the carbon chain length and both the surface diffusion activation energy E_{dif} and desorption activation barrier E_{des}. These studies also demonstrated that the surface corrugation ratio, $\Omega = E_{dif}/E_{des}$, was constant at $\Omega \simeq 0.3$. This constancy indicates that the modulation of the potential parallel to the surface is similar for all the *n*-alkanes on Ru(001).

This study of *n*-alkanes on Ru(001) builds on previous LITD surface diffusion studies of hydrogen[8-14] and carbon monoxide[15,16] on Ru(001). These earlier investigations explored the surface diffusion of model chemisorption systems composed of atomic and molecular species. The present study extended the previous work and explored a series of physisorbed molecular species. The results suggested that a linear scaling exists between E_{dif} and E_{des} for a homologous series of physisorbed molecules.

II. EXPERIMENTAL

In the LITD surface diffusion experiment,[8,17] an initial laser pulse is used to heat a well-defined area on a surface. The laser heating produces a rapid temperature jump that is large enough to desorb the adsorbates within the heated area.[18,19] After a time delay, a second identical probe laser pulse heats the same area and desorbs the adsorbates that have diffused into the initially evacuated region from the surrounding surface.

The desorption flux at each delay time corresponds to the amount of diffusional refilling. The time-dependent refilling signals are fit using the appropriate solution to Fick's second law to determine the surface diffusion coefficient.[8] This prepare-and-probe LITD experimental procedure has been successfully employed in numerous recent studies to measure surface diffusion on single-crystal metal surfaces.[8-16,20-24]

The experimental setup for these LITD measurements of surface diffusion has been described previously.[8] Briefly, the experiments were performed in an ion-pumped UHV chamber with background pressures below 3×10^{-10} Torr. Analysis of surface cleanliness and surface order was carried out with Auger electron spectroscopy (AES) using a single-pass cylindrical mirror analyzer (CMA) and low energy electron diffraction (LEED) spectrometry.

The surface cleaning procedure involved exposing the

[a] Present address: IBM Almaden Research Center, San Jose, California 95193.
[b] Present address: Department of Chemistry, College of the Holy Cross, Worcester, Massachusetts 01610.

 0021-9606/90/085136-08$03.00

Ru(001) crystal to O_2 and cycling the crystal temperature between 1100 and 1370 K for two to three cycles.[8-16] The flow of oxygen was stopped while the crystal was at 1370 K. Repeated flashing to 1600 K was required to remove excess oxygen. No traces of carbon or oxygen could be detected using AES after this procedure. The surface cleanliness was also monitored using CO temperature programmed desorption (TPD) peak temperatures as discussed previously.[15]

A TEM-00 Q-switched Nd:phosphate glass laser producing pulselengths of 110–130 ns with Gaussian spatial profiles was employed.[8] The reasons for using longer pulselengths have been discussed previously.[25] In the present study, the laser pulse energy before entering the UHV chamber was approximately 0.15 mJ/pulse. The pulses were focused by a 65 cm focal length lens to give a Gaussian spatial profile of 120 μm (FWHM) at the focus of the lens.

The surface was positioned at the focus of the lens. The angle between the incoming laser pulses and the surface normal was 54°. Consequently, the desorption areas were elliptical with an aspect ratio of 1.7. The dimensions of the desorption spots using the spatial autocorrelation method[17] were approximately 155 μm in diameter along the minor axis and 260 μm along the major axis.

Gases were adsorbed on the Ru(001) crystal using a glass multichannel capillary array doser attached to a variable leak valve. The doser was positioned approximately 1.5 cm from the surface. The gases were adsorbed uniformly to within $\pm$ 10% across the entire Ru(001) surface as measured by LITD spatial analysis. Each *n*-alkane was dosed with the Ru(001) crystal at a different temperature: 100 K for propane, 125 K for *n*-butane, 150 K for *n*-pentane and 180 K for *n*-hexane. After every experiment, the Ru(001) surface was cleaned by exposing the Ru crystal to a 2–4 L oxygen dose at 1300 K and, subsequently, heating the crystal to 1600 K.[8-16]

For the diffusion experiments, each desorption area was prepared with a sequence of five consecutive pulses to ensure complete desorption inside the area.[25] Each of the areas was probed with a second sequence of identical laser pulses at time delays ranging from 15 to 1000 s. As mentioned earlier, the size of the desorption area was measured for each *n*-alkane after each experiment using the spatial autocorrelation method.[17] Piezoelectric translators moved the laser beam on the surface with an accuracy of $\pm$ 0.5 μm.

III. RESULTS

A. Surface diffusion measurements

1. Temperature dependence

The normalized diffusional refilling data for *n*-hexane at $\Theta = 0.2\ \Theta_{sat}$ for a variety of temperatures are displayed in Fig. 1. Θ_{sat} is the coverage of the saturated *n*-hexane monolayer and should correspond to a coverage of approximately $\Theta_{sat} \simeq 2.2\times10^{14}$ molecules/cm^2.[26,27] The expected refilling curves corresponding to constant diffusion coefficients were fit to the experimental data and are shown as solid lines. The data points are not averages from many runs, but are results from single prepare-and-probe sequences at various delay times. Moreover, the data for the lower temperatures in Fig. 1 extend to times longer than 400 s. The time scale ends at 400 s for clarity in presentation.

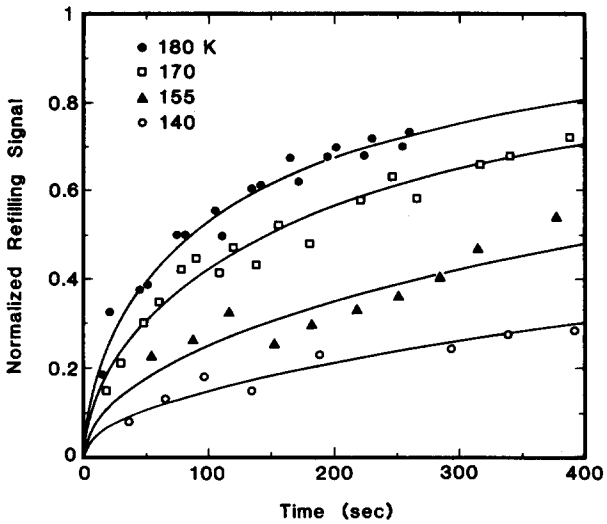

FIG. 1. Diffusional refilling data for *n*-hexane on Ru(001) at various temperatures at $\Theta = 0.2\Theta_{sat}$. Solid lines represent refilling curves corresponding to constant surface diffusion coefficients.

To determine the value of the surface diffusion coefficient, the size of the desorption area must be known. Measurements of the desorption holesize for *n*-hexane at 170 K using the spatial autocorrelation method[17] are displayed in Fig. 2. In the spatial autocorrelation method, the initial desorption signal is recorded. The laser beam is then translated a distance ΔX on the surface. Desorption from the region outside of the area of the initial desorption region gives rise to the second desorption signal.[17] The normalized LITD signal is defined as the ratio between the second desorption signal and the initial desorption signal.

The data shown in Fig. 2 yield a holesize of 155 μm along the minor axis. Similar measurements yield a holesize of 260 μm along the major axis. Given this holesize, surface diffusion coefficients can be assigned to the diffusional refilling data in Fig. 1. The Arrhenius plot for the temperature-dependent surface diffusion coefficient for *n*-hexane is displayed in Fig. 3. The slope yields an activation energy for

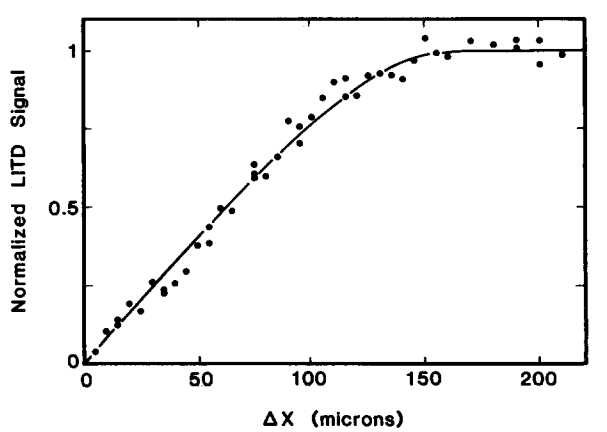

FIG. 2. Determination of the desorption holesize for *n*-hexane at 170 K using the spatial autocorrelation method. These measurements yield a holesize of 155 μm along the minor axis.

surface diffusion of $E_{dif} = 4.8 \pm 0.2$ kcal/mol. Likewise, the y intercept yields a diffusion preexponential of $D_0 = 1.6 \times 10^{-1 \pm 0.1}$ cm^2/s. The uncertainties represent the standard deviation of the slope and y-intercept obtained from a linear regression analysis of the data.

Normalized diffusional refilling data were obtained vs temperature for the *n*-alkanes on Ru(001) at approximately $\Theta = 0.2\,\Theta_{sat}$. Refilling curves similar to Fig. 1 were obtained for all the *n*-alkanes on Ru(001). For example, temperature-dependent refilling curves for *n*-butane are displayed in Fig. 4. The coverage of a saturated *n*-butane monolayer should correspond to a coverage of approximately $\Theta_{sat} \simeq 3.0 \times 10^{14}$ molecules/cm^2.[26,27] All the refilling curves were fit extremely well using constant diffusion coefficients.

Desorption holesizes for all the *n*-alkanes on Ru(001) were measured each day after every set of experiments. These holesizes allowed absolute diffusion coefficients to be assigned. All of the temperature-dependent surface diffusion coefficients for the *n*-alkanes on Ru(001) are summarized by the Arrhenius plot shown in Fig. 5.

The surface diffusion activation energies increased nearly linearly with the size of the carbon chain as shown in Fig. 6(a). In contrast, the diffusion preexponential remained nearly constant at $D_0 \simeq 0.15$ cm^2/s for all of the *n*-alkanes as displayed in Fig. 6(b). The Arrhenius parameters for the surface diffusion of *n*-alkanes on Ru(001) are also listed in Table I.

2. Coverage dependence

If adsorbate–adsorbate interactions are present, the surface diffusion coefficient can be coverage dependent.[2,3,28] These adsorbate–adsorbate interactions can be measured by LITD diffusional refilling experiments[28] as has been recently demonstrated for CO on Ru(001).[15,16] The coverage dependence of the surface diffusion coefficients was measured for all the *n*-alkanes. Figure 7 displays the surface diffusion coefficient versus coverage for *n*-hexane at 170 K and propane at 110 K. The error bars were determined by the largest and smallest diffusion coefficients that bracketed all the data points from individual prepare-and-probe experiments.

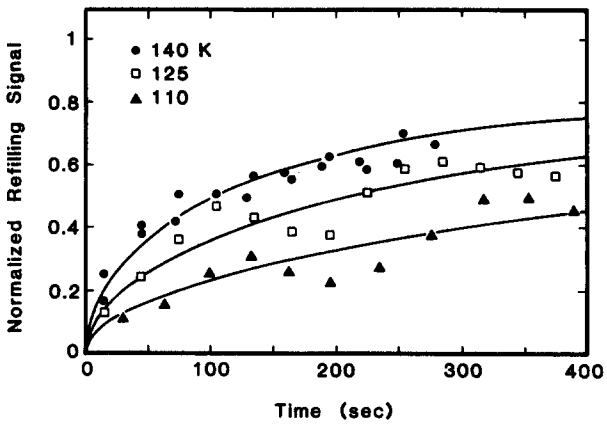

FIG. 4. Diffusional refilling data for *n*-butane on Ru(001) at various temperatures at $\Theta = 0.2\Theta_{sat}$. Solid lines represent refilling curves corresponding to constant surface diffusion coefficients.

The surface diffusion coefficients for all the *n*-alkanes on Ru(001) were coverage independent. As an additional check on the coverage independence of the surface mobility, the temperature dependence of the surface diffusion coefficient at saturation coverage was measured for *n*-pentane. The Arrhenius parameters for the surface diffusion coefficient of *n*-pentane on Ru(001) were identical at both low and saturation coverage.

B. Thermal desorption measurements

The desorption activation energies for the *n*-alkanes were measured using the variation of heating rates method.[29] Figure 8 displays the temperature programmed desorption (TPD) spectra for *n*-hexane as a function of heating rate. The TPD spectra have been rescaled for clarity in presenta-

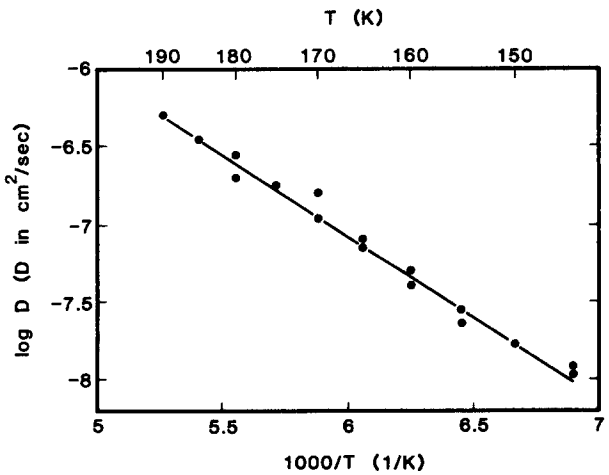

FIG. 3. Arrhenius plot of the surface diffusion coefficients for *n*-hexane on Ru(001) at $\Theta = 0.2\Theta_{sat}$. The measured diffusion kinetic parameters were $E_{dif} = 4.8 \pm 0.2$ kcal/mol and $D_0 = 1.6 \times 10^{-1 \pm 0.1}$ cm^2/s.

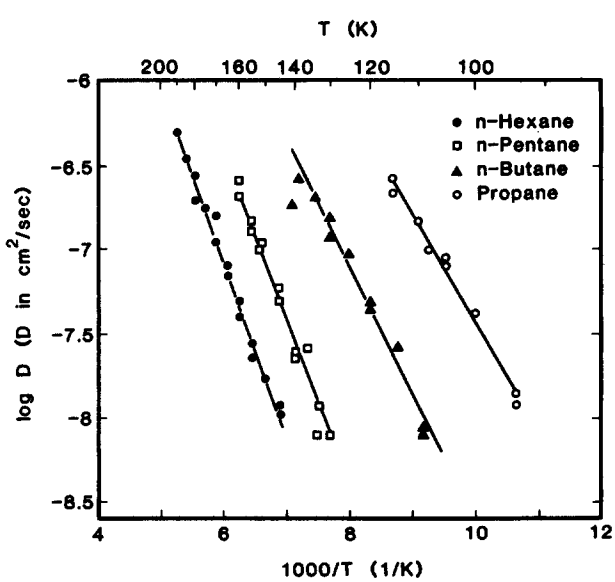

FIG. 5. Arrhenius plots of the surface diffusion coefficients for propane, *n*-butane, *n*-pentane, and *n*-hexane on Ru(001) at $\Theta = 0.2\Theta_{sat}$.

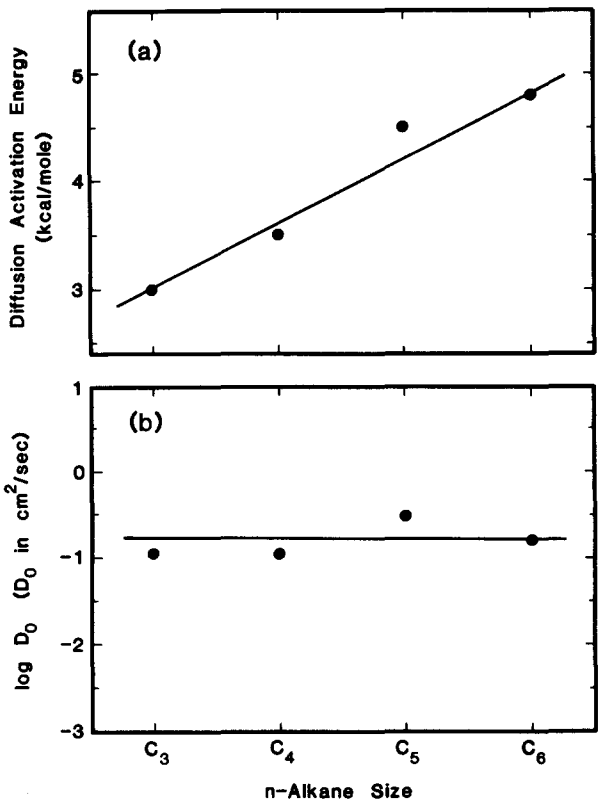

FIG. 6. Kinetic parameters for the surface diffusion of *n*-alkanes on Ru(001) vs carbon chain length.

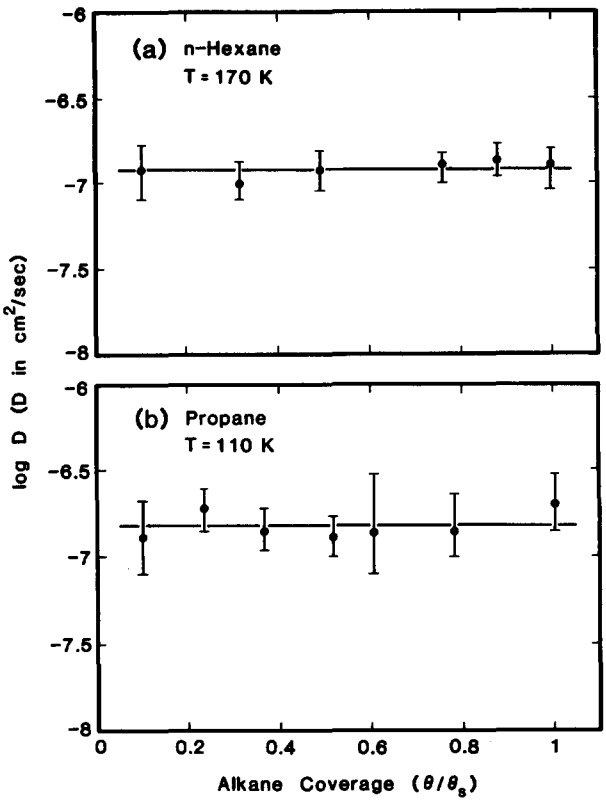

FIG. 7. Coverage dependence of the surface diffusion coefficient on Ru(001) for (a) *n*-hexane at 170 K and (b) propane at 110 K.

tion. The TPD spectra were analyzed using the standard Redhead analysis[29] as shown in Fig. 9. The desorption activation energy, $E_{des} = 15.0 \pm 0.5$ kcal/mol, was obtained from the slope of this Redhead analysis. Likewise, a desorption preexponential of $\upsilon_{des} = 8.0 \times 10^{14 \pm 0.1}\ s^{-1}$ was derived from the y intercept and the slope. The uncertainties represent the standard deviation of the slope and y intercept obtained from a linear regression analysis of the data.

The heating rate variation method was applied to all the *n*-alkanes on Ru(001). TPD spectra with peaks at higher temperatures corresponding to faster heating rates were obtained for all the *n*-alkanes. Figure 10 shows the Redhead analysis of this thermal desorption data for the various *n*-alkanes.

The desorption activation energies increased nearly linearly with the size of the carbon chain as shown in Fig. 11(b). In contrast, the desorption preexponentials remained nearly constant at approximately $\upsilon_{des} \simeq 1 \times 10^{15}\ s^{-1}$ for all of the *n*-alkanes. The Arrhenius parameters for the thermal desorption of *n*-alkanes from Ru(001) are given in Table I.

The three largest *n*-alkanes, *n*-butane, *n*-pentane, and *n*-hexane, formed stable multilayers on Ru(001) above 95 K. The zero-order desorption of these multilayers was monitored using TPD studies with multilayer coverages of $\Theta = 8$–10 ML. At a heating rate of $\beta = 2$ K/s, the multilayers desorbed at 120 K for *n*-butane, 134 K for *n*-pentane, and 150 K for *n*-hexane.

C. Additional measurements

LEED measurements attempted to detect ordered overlayers of *n*-alkanes on Ru(001). In accordance with measurements of cycloalkanes on Ru(001),[30–32] no new diffraction spots were observed. LEED measurements of hydrocarbons are difficult and LEED patterns for *n*-alkanes on single-crystal metal surfaces have only been observed on

TABLE I. Summary of the surface diffusion and desorption kinetic parameters, peak desorption temperatures, and corrugation ratios for the *n*-alkanes on Ru(001).

n-Alkane	E_{dif} (kcal/mol)	D_0 (cm^2/s)	E_{des} (kcal/mol)	υ_{des} (sec^{-1})	T_{peak} (K)	Ω
Propane	3.0	0.11	11.0	3.1×10^{16}	143	0.27
n-Butane	3.5	0.11	11.9	3.6×10^{15}	170	0.29
n-Pentane	4.5	0.30	13.8	1.8×10^{15}	198	0.32
n-Hexane	4.8	0.16	15.0	8.0×10^{14}	225	0.32

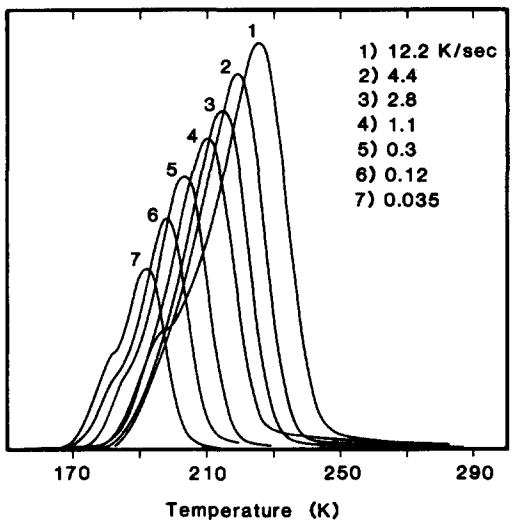

FIG. 8. Temperature programmed desorption (TPD) spectra for *n*-hexane on Ru(001) as a function of heating rate. The TPD spectra have been scaled for clarity in presentation.

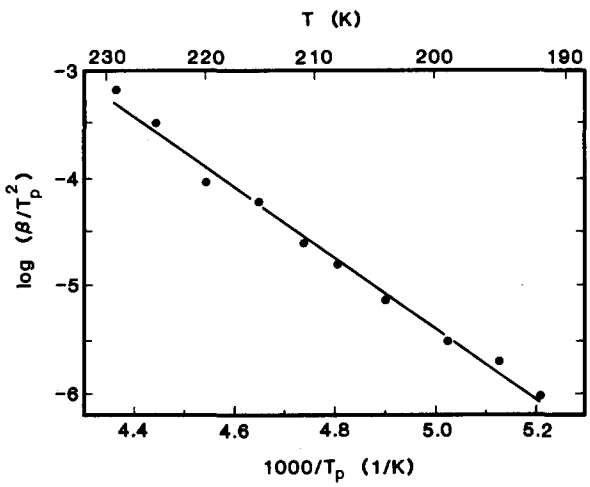

FIG. 9. Redhead analysis of the TPD spectra for *n*-hexane on Ru(001) as a function of heating rate. The measured desorption kinetic parameters were $E_{des} = 15.0 \pm 0.5$ kcal/mol and $\nu_{des} = 8.0 \times 10^{14 \pm 0.1}$ s^{-1}.

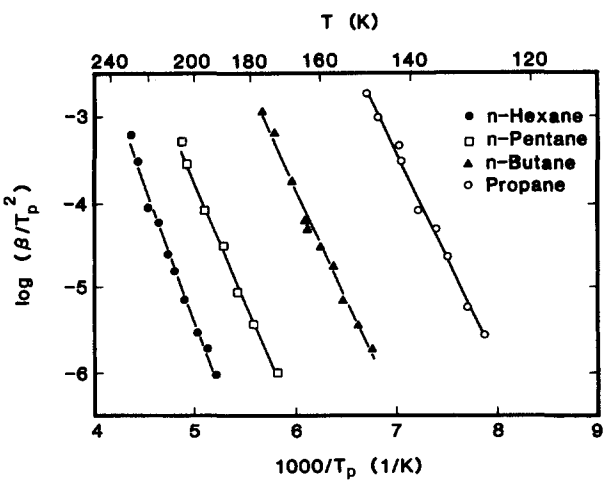

FIG. 10. Redhead analysis of the TPD spectra for propane, *n*-butane, *n*-pentane, and *n*-hexane on Ru(001) as a function of heating rate.

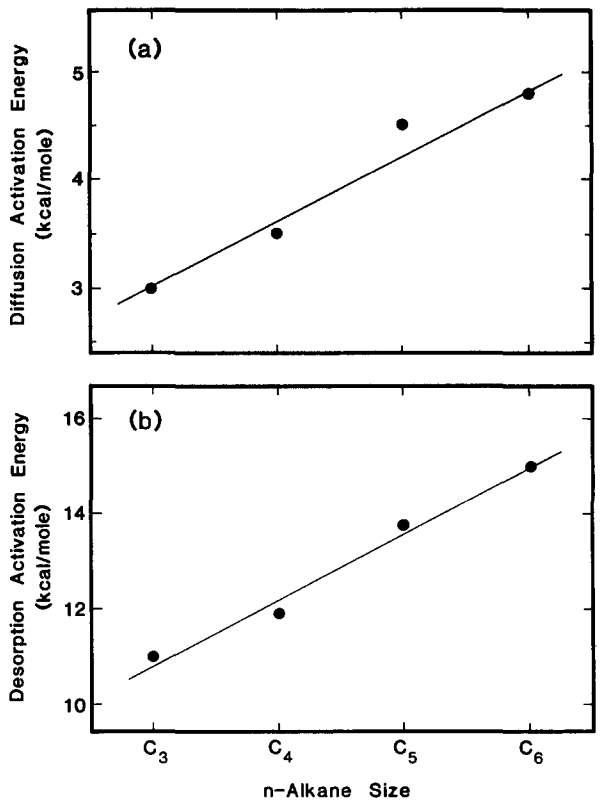

FIG. 11. Linear scaling of the (a) surface diffusion activation energy and (b) desorption activation energy as a function of *n*-alkane size.

Pt(111)[26] and Ag(111).[33] Hydrocarbons are believed to be very susceptible to electron-induced decomposition and desorption.[26,33]

Quantitative measurements of surface carbon determined if any of the *n*-alkanes decomposed on the Ru(001) surface. The amount of carbon on Ru(001) is difficult to measure quantitatively with AES. Consequently, oxygen uptake experiments were performed to measure any possible carbon on the Ru(001) surface. A detailed description of the oxygen uptake experiments has been given earlier.[9,34] Only negligible traces of carbon could be detected by these measurements. The carbon coverage on Ru(001) after the desorption of a saturation exposure of any of the *n*-alkanes was $\Theta_c \leqslant 0.02$ ML.

IV. DISCUSSION

A. Coverage independent diffusion

Measurements of surface diffusion and desorption provide direct information about the parallel and perpendicular surface potentials.[1-3] At low adsorbate coverages, the activation energies are dominated by the adsorbate–surface potential energy. As the adsorbate coverage is increased, adsorbate-adsorbate interactions may become important and can influence surface diffusion.[2,3,35] The surface diffusion of CO on Ru(001) was a dramatic example where repulsive nearest-neighbor interactions significantly influenced CO surface mobility.[15,16]

In the case of the *n*-alkanes on Ru(001), Fig. 7 reveals that the surface diffusion coefficients are coverage independent. This behavior indicates that the parallel surface potential is dominated by adsorbate–surface interactions. The absence of any LEED patterns for the *n*-alkanes on Ru(001) is also consistent with the absence of strong adsorbate–adsorbate interactions.

The TPD spectra for the *n*-alkanes on Ru(001) vs coverage displayed simple, coverage-independent first-order desorption kinetics. Similar coverage-independent desorption kinetics have also been observed for butane and pentane on Pt(111).[36] In agreement with the surface diffusion measurements, this behavior indicates that the perpendicular surface potential is dominated by adsorbate–surface interactions.

In addition, multilayer desorption temperatures are observed that are considerably less than the monolayer desorption temperatures. For example, the multilayer and monolayer desorption temperatures for *n*-hexane on Ru(001) were 150 and 225 K, respectively. This behavior is also consistent with small adsorbate–adsorbate interactions compared with adsorbate-surface interactions.

B. Diffusion mechanism and linear scaling

For the simple case of an adatom diffusing over a surface, the diffusion mechanism is generally assumed to involve an atom that resides in a specific minimum energy binding site. This binding site could be a threefold or fourfold hollow site on a hexagonal or square lattice surface. The adatom then transits over a bridge site into the neighboring minimum energy binding site.[8,17,37] Consequently, the surface diffusion activation energy is approximately the potential energy difference between the binding site and the bridge site.

This simple picture for adatom diffusion serves as a model, but cannot be applied easily to the diffusion of polyatomic molecules. The *n*-alkanes on Ru(001) may reside in many surface configurations that may have energies near the minimum energy configuration. Likewise, multiple transition states may be present during the translation of the *n*-alkanes on the Ru(001) surface. Thus the observed diffusion activation energy is probably an average over all the initial surface configurations and the various possible transitional configurations.

Despite the lack of clearly defined binding and transition states, the diffusion and desorption data reveal general trends. For example, the activation energies for diffusion and desorption both scale nearly linearly with the carbon chain length as shown in Fig. 11. Linear relationships between desorption activation energies and carbon chain length have been observed earlier for *n*-alkanes on Cu(100)[38] and cycloalkanes on Ru(001).[30] Likewise, LEED studies of *n*-alkanes on Pt(111)[26] and Ag(111)[33] are consistent with a progressively increasing adsorption energy with alkane size.

Recent theoretical calculations also predict a nearly linear scaling between adsorption energy and carbon chain length for *n*-alkanes physisorbed on Ru(001).[39] The calculations reveal that physisorption interactions alone are sufficient to explain the measured desorption activation energies on Ru(001). In addition, the carbon chains are predicted to lie parallel to the Ru(001) surface in an all-*trans* configuration. The theoretical results are based on a simple summing of Lennard-Jones pair potentials for carbon-ruthenium and hydrogen-ruthenium interactions with the attractive well depth determined by dispersion forces.[39]

A surface diffusion activation barrier that scales linearly with the carbon chain length is more surprising and revealing. This linear scaling would *not* be expected if the alkanes moved segmentally or by "reptation," i.e., the snake-like wiggling of individual sections of the molecule.[40] According to the reptation model from polymer physics, the diffusion coefficients for polymers are inversely proportional to the square of the polymer length, $D \propto 1/n^2$.[40] The reptation model also predicts that the diffusion activation energy is the same for polymers with different lengths and only the diffusion preexponential varies.

Measurements of the diffusion of linear hydrocarbons through bulk polyethylene reveal that the diffusion agrees well with the reptation model for chains longer than 30-CH_2 units.[41] In contrast, the diffusion does not obey the reptation model for chains shorter than 30 carbons units. In the words of Klein and Briscoe, "In terms of the previous reptilian analogy, the wriggling snake has become so short that ... its motion is more a series of hops in which all of the snake is involved."[41]

Only simple qualitative comparisons can be made between bulk diffusion through an entangled polymer and diffusion on a single-crystal metal surface. However, the data presented in Fig. 11 and in Table I indicates that the reptation model is inconsistent with the diffusion behavior of small, straight-chain alkanes on Ru(001). On the other hand, the linear scaling between both the diffusion and desorption activation barriers and the carbon chain length argues that the *n*-alkanes move in a concerted fashion on Ru(001).

C. Model for linear scaling

The surface diffusion data for *n*-alkanes on Ru(001) suggests that the mechanism for surface diffusion must involve the concerted motion of the entire molecule. The simplest concerted motion model assumes that the surface diffusion activation energy is proportional to N, the carbon length of the *n*-alkane, $E_{dif} = aN$. To reproduce the measured diffusion activation energies, a fit of this simple model to the data yields $a = 0.85$ kcal/mol per carbon unit.

Another simple concerted motion model allows the methyl and methylene groups to have different diffusion activation energies, e.g., $E_{dif} = bN_{CH_3} + cN_{CH_2}$. Using this concerted motion model, the measured diffusion activation energies can be modeled extremely well with $b = 1.21$ kcal/mol per methyl unit and $c = 0.60$ kcal/mol per methylene unit. The fit of this model to the measured surface diffusion activation energies is shown by the solid line in Fig. 6(a).

The diffusion preexponential D_0 can also be modeled by assuming that D_0 scales with the hopping attempt frequency. This hopping attempt frequency should be related to s, the frustrated translational velocity on the surface. Consequent-

ly, given that $2kT = ms^2$ and $s = (2kT/m)^{1/2}$, D_0 should be proportional to $(T/m)^{1/2}$, where T is the temperature and m is the mass.

The surface diffusion experiments for the larger carbon chains were performed at higher temperatures. Consequently, $D_0 \propto (T/m)^{1/2}$ remains fairly constant during the experiments for the various *n*-alkanes because increasing both temperature and mass produce compensating changes in $D_0 \propto (T/m)^{1/2}$. A comparison between $D_0 \propto (T/m)^{1/2}$ and the experimental surface diffusion preexponentials is shown by the solid line in Fig. 6(b). The predicted D_0 values were evaluated at the surface temperature corresponding to $D = 5\times10^{-8}$ cm^2/s. Likewise, these predicted values were normalized using the measured D_0 value for *n*-hexane. The agreement between the predicted and measured D_0 values is extremely good.

The concerted motion model for E_{dif} and the frustrated translational velocity model for D_0 can be combined to yield an expression for the total diffusion coefficient:

$$D = A(T/m)^{1/2}\exp[-(bN_{CH_3} + cN_{CH_2})/RT].$$

A is a proportionality constant equal to $A = 0.10$ cm^2/s if the units of T and m are Kelvin and amu, respectively. This expression for the total diffusion coefficient is in excellent agreement with the experimental surface diffusion data for all the *n*-alkanes on Ru(001).

D. Diffusion and desorption preexponentials

Despite the excellent agreement for the concerted motion model, the magnitudes of the diffusion preexponentials are larger than expected based on a simple one site jump model. According to random walk theory, $D_0 = r^2v/4$, where r is the jump length and v is the attempt frequency. The jump length is initially assumed to correspond to a single site jump between adjacent threefold sites on Ru(001). The attempt frequency can be estimated by $v = s/l$ where s is the frustrated translational velocity and l is the effective confinement length for the alkanes in their surface binding wells.

Using values of $l \simeq 1$ Å, $r = 1.4$ Å, $m = 65$ amu, and $T = 130$ K, values of $v = 1.8\times10^{12}$ s^{-1} and $D_0 = 8.9\times10^{-5}$ cm^2/s were obtained. Notice that the measured diffusion preexponentials are approximately 10^3 times larger than the predicted values. These large values may be revealing that the *n*-alkanes are moving more than one threefold-to-threefold site length in a single jump. Multiple site jumps have been suggested by recent molecular dynamics simulations.[42] Jump lengths of $r = 40$–50 Å are required to match the measured D_0 values assuming that $v = 1.8\times10^{12}$ s^{-1}.

Using the Arrhenius parameters for surface diffusion, the diffusion coefficients can be calculated at temperatures outside the range where the diffusion experiments were performed. At the temperatures where each of the *n*-alkanes desorb, the diffusion coefficients were all calculated to be approximately $D \simeq 3\times10^{-6}$ cm^2/s. This surprising observation indicates that all the *n*-alkanes have similar surface mobilities when they desorb from Ru(001).

The desorption preexponential is related to the entropy that the molecule has gained in going from the adsorbed state to the desorbed state. If the *n*-alkanes all have similar diffusion coefficients when they desorb from Ru(001), the change in entropy upon desorption for each of the *n*-alkanes will be comparable. In agreement with this picture, Table I indicates that the desorption preexponentials for the various *n*-alkanes on Ru(001) are very similar.

E. Surface corrugation

The corrugation ratio, $\Omega = E_{dif}/E_{des}$ is defined as the ratio of the diffusion activation energy E_{dif} to the desorption activation energy E_{des}. The corrugation ratio provides a measure of the modulation of the surface potential parallel to the surface. Table I reveals that the measured corrugation ratios are nearly constant at $\Omega \simeq 0.3$ for all the *n*-alkanes on Ru(001). This constant corrugation ratio indicates that E_{dif} and E_{des} both scale linearly with the carbon chain length as displayed in Fig. 11.

The linear scaling between E_{dif} and E_{des} would not be expected unless the *n*-alkanes shared similar configurations, binding orientations, and diffusion mechanisms on Ru(001). The constancy of the corrugation ratio argues that the *n*-alkanes are all in a rigid, probably all-*trans*, configuration parallel to the Ru(001) surface. An all-*trans* configuration is the lowest energy orientation in the gas phase. An all-*trans* configuration on the surface is also predicted by theoretical calculations[39] and is supported by previous LEED[26] and IR[43] studies of *n*-alkanes on Pt(111).

The constancy of the corrugation ratio also suggests a universal scaling of the surface potential for *n*-alkanes on Ru(001). As the carbon chain length and the adsorption energy increases, the surface diffusion activation energy also increases. This behavior is reminiscent of the universal scaling suggested by laterally averaged physisorption[44] and chemisorption[45] surface potentials.

Additional surface diffusion experiments are needed to determine if physisorbed hydrocarbon molecules all display a constant corrugation ratio on metal surfaces. We note that earlier[46] and more recent[47] measurements of cycloalkanes on Ru(001) displayed a constant surface corrugation ratio of $\Omega \simeq 0.3$. Recent surface diffusion measurements of pentane isomers on Ru(001) have also revealed a constant corrugation ratio of $\Omega \simeq 0.3$.[48]

Constant corrugation ratios have been observed previously for various chemisorbed systems. A constant corrugation ratio of $\Omega \simeq 0.1$ has been measured for the 5*d* transition metal atoms on W(110).[49] Likewise, hydrogen on Ru(001),[8,10,11] Rh(111)[24] and Ni(100)[17,22] has displayed a nearly constant corrugation ratio of $\Omega \simeq 0.07$. Numerous other chemisorbed adsorbates have also revealed corrugation ratios in the range $\Omega = 0.1$ to $\Omega = 0.4$.[15,21,24,50]

A surface corrugation ratio of $\Omega \simeq 0.3$ for the *n*-alkanes on Ru(001) is higher than the expected ratio of $\Omega \simeq 0.12$–0.15 predicted by theoretical calculations for physisorbed species.[39,51] However, Xe on W(110) displayed a similar corrugation ratio of $\Omega = 0.25$.[52] High corrugation ratios may indicate that steps or defects are affecting surface diffusion. Alternatively, simple physisorption calculations may

not be adequate to define the activation barriers for surface diffusion. Measurements of diffusion on stepped Ru(001) surfaces are planned to resolve these questions.

V. CONCLUSION

The surface diffusion coefficients for propane, *n*-butane, *n*-pentane, and *n*-hexane on Ru(001) were measured using laser-induced thermal desorption (LITD) techniques. The surface diffusion coefficients for these *n*-alkanes displayed Arrhenius behavior. The surface diffusion activation energies increased linearly with carbon chain length from $E_{dif} = 3.0 \pm 0.1$ kcal/mol for propane to $E_{dif} = 4.8 \pm 0.2$ kcal/mol for *n*-hexane.

In contrast, the surface diffusion preexponentials remained nearly constant at $D_0 \simeq 0.15$ cm^2/s. The magnitude of D_0 was larger than expected based on a simple one site jump model. These large D_0 values suggested that the *n*-alkanes may be moving more than one site per jump. Surface diffusion measurements also revealed that the diffusion coefficients for the *n*-alkanes were coverage independent. This behavior indicated that the parallel surface potential is dominated by adsorbate–surface interactions.

A simple concerted motion model was constructed to explain the linear scaling between the surface diffusion activation barrier and the carbon chain length. The activation barriers were shown to fit well to $E_{dif} = bN_{CH_3} + cN_{CH_2}$ where $b = 1.21$ kcal/mol per methyl unit and $c = 0.6$ kcal/mol per methylene unit. Likewise, the diffusion preexponentials were observed to be proportional to $D_0 \alpha (T/m)^{1/2}$.

The surface corrugation ratio Ω was defined as the ratio of the diffusion activation energy to the desorption activation energy, $\Omega = E_{dif}/E_{des}$. The surface corrugation ratio was remarkably constant at $\Omega \simeq 0.3$ for all the *n*-alkanes on Ru(001). This constancy indicated a linear scaling between the diffusion activation energy and the desorption activation energy. This constant corrugation ratio also suggested that the *n*-alkanes move with a rigid, probably all-*trans*, configuration parallel to the Ru(001) surface.

ACKNOWLEDGMENTS

This work was supported by the National Science Foundation under Grants No. CHE-8514102 and CHE-8908087. Some of the equipment utilized in this work was provided by the NSF-MRL program through the Center for Materials Research at Stanford University. M.V.A. thanks the Eastman Kodak Company for a Kodak Graduate Fellowship. S.M.G. acknowledges the National Science Foundation for a Presidential Young Investigator Award and the A.P. Sloan Foundation for a Sloan Research Fellowship.

[1]G. Ehrlich and K. J. Stolt, Ann. Rev. Phys. Chem. **31**, 603 (1980).
[2]D. A. King, J. Vac. Sci. Technol. **17**, 241 (1980).
[3]D. A. King, in *Chemistry and Physics of Solid Surfaces*, Vol. 2 (CRC, Boca Raton, 1979).
[4]P. Bileon and W. M. H. Sachtler, Adv. Catalysis **30**, 165 (1981).
[5]M. A. Vannice, J. Catalysis **37**, 449 (1975).
[6]M. A. Vannice, J. Catalysis **37**, 462 (1975).
[7]M. A. Vannice, Catalysis Rev. **14**, 153 (1976).
[8]C. H. Mak, J. L. Brand, A. A. Deckert, and S. M. George, J. Chem. Phys. **85**, 1676 (1986).
[9]C. H. Mak, B. G. Koehler, J. L. Brand, and S. M. George, J. Chem. Phys. **87**, 2340 (1987).
[10]C. H. Mak, J. L. Brand, B. G. Koehler, and S. M. George, Surf. Sci. **191**, 108 (1987).
[11]C. H. Mak, J. L. Brand, B. G. Koehler, and S. M. George, Surf. Sci. **188**, 312 (1987).
[12]J. L. Brand, A. A. Deckert, and S. M. George, Surf. Sci. **194**, 457 (1988).
[13]C. H. Mak, A. A. Deckert, and S. M. George, J. Chem. Phys. **89**, 5242 (1988).
[14]C. H. Mak, B. G. Koehler, and S. M. George, J. Vac. Sci. Technol. A **6**, 856 (1988).
[15]A. A. Deckert, J. L. Brand, M. V. Arena, and S. M. George, Surf. Sci. **208**, 441 (1989).
[16]A. A. Deckert, J. L. Brand, M. V. Arena, and S. M. George, J. Vac. Sci. Technol. A **6**, 794 (1988).
[17]S. M. George, A. M. DeSantolo, and R. B. Hall, Surf. Sci. **159**, L425 (1985).
[18]J. P. Cowin, D. J. Auerbach, C. Becker, and L. Warton, Surf. Sci. **78**, 545 (1978).
[19]G. Wedler and H. Ruhmann, Surf. Sci. **121**, 464 (1982).
[20]R. Viswanathan, D. R. Burgess, Jr., P. C. Stair, and E. Weitz, J. Vac. Sci. Technol. **20**, 605 (1982).
[21]B. Roop, S. A. Costello, D. R.Mullins, and J. M. White, J. Chem. Phys. **86**, 3003 (1987).
[22]D. R. Mullins, B. Roop, and J. M. White, Chem. Phys. Lett. **129**, 511 (1986).
[23]E. G. Seebauer, A. C. F. Kong, and L. D. Schmidt, J. Vac. Sci. Technol. A **5**, 464 (1987).
[24]E. G. Seebauer, A. C. F. Kong, and L. D. Schmidt, J. Chem. Phys. **88**, 6597 (1988).
[25]J. L. Brand and S. M. George, Surf. Sci. **167**, 341 (1986).
[26]L. E. Firment and G. A. Somorjai, J. Chem. Phys. **66**, 2901 (1977).
[27]A. Gavezzotti, M. Simonetta, M. A. Van Hove, and G. A. Somarjai, Surf. Sci. **154**, 109 (1985).
[28]C. H. Mak and S. M. George, Surf. Sci. **172**, 509 (1986).
[29]P. A. Redhead, Vacuum **12**, 203 (1962).
[30]T. E. Madey and J. T. Yates, Jr., Surf. Sci. **76**, 397 (1978).
[31]T. E. Felter, F. M. Hoffmann, P. A. Thiel, and W. H. Weinberg, Surf. Sci. **130**, 163 (1983).
[32]F. M. Hoffmann, T. E. Felter, P. A. Thiel, and W.H. Weinberg, Surf. Sci. **130**, 173 (1983).
[33]L. E. Firment and G. A. Somorjai, J. Chem. Phys. **69**, 3940 (1978).
[34]S. K. Shi and J. M. White, J. Chem. Phys. **73**, 5889 (1980).
[35]M. Bowker and D. A. King, Surf. Sci. **71**, 583 (1978)
[36]M. Salmeron and G. A. Somorjai, J. Phys. Chem. **85**, 3835 (1981).
[37]C. H. Mak and S. M. George, Chem. Phys. Lett. **135**, 381 (1987).
[38]B. A. Sexton and A. E. Hughes, Surf. Sci. **140**, 227 (1984).
[39]M. V. Arena and S. M. George (in preparation).
[40]P. G. de Gennes, *Scaling Concepts in Polymer Physics* (Cornell University, Ithaca, 1979).
[41]J. Klein and B. J. Briscoe, Proc. R. Soc. London Ser. A **365**, 53 (1979).
[42]D. J. Doren (unpublished results).
[43]M. A. Chesters, P. Gardner, and E. M. McCash, Surf. Sci. **209**, 89 (1989).
[44]G. Vidali, M. W. Cole, and J. R. Klein, Phys. Rev. B **28**, 3064 (1983).
[45]J. Ferrante, J. R. Smith, and J. H. Rose, Phys. Rev. Lett. **50**, 1385 (1983).
[46]C. H. Mak, B. G. Koehler, and S. M. George, J. Vac. Sci. Technol. A **6**, 856 (1988).
[47]M. V. Arena, J. L. Brand, A. A. Deckert, and S. M. George (in preparation).
[48]M. V. Arena, J. L. Brand, A. A. Deckert, and S. M. George, J. Phys. Chem. (submitted).
[49]A. G. Naumovets and Y. S. Vedula, Surf. Sci. Rep. **4**, 365 (1985).
[50]G. Ehrlich in: *Chemistry and Physics of Solid Surfaces*, Vol. III, edited by R. Vanselow and W. England (CRC, Boca Raton, 1982), p. 391.
[51]F. O. Goodman, Phys. Rev. **164**, 1113 (1967).
[52]J.-R. Chen and R. Gomer, Surf. Sci. **94**, 456 (1980).